# MULTI-PHYSICS SIMULATION AND TRAJECTORY OPTIMIZATION IN LASER WELDING OF COPPER HAIRPIN WINDINGS

P. RANA*, M. SREEJITH**, C. OBERGFELL*,***, M. KAISER*,****, P. MAYR***

**Mercedes Benz AG, Deutschland*
***Mercedes Benz Research and Development, India*
****TU München*
*****TU Braunschweig*
*pulkit.rana@mercedes-benz.com*

*DOI 10.3217/978-3-99161-089-2-005, license CC BY 4.0*


ABSTRACT

The development of a digital process chain for laser welding copper hair pin windings is essential for advancing the manufacturing of components used in electrical vehicles, electronic devices, and energy storage systems. Copper's high thermal conductivity and low infrared light absorption can lead to process instabilities during laser welding, such as melt pool spatter and porosity, resulting in inconsistent weld quality. Understanding the physics involved in laser welding - from keyhole and melt pool formation to the solidification of the melt pool - is crucial. This study employs Cradle CFD for multi-physics analysis to simulate and optimize the laser welding process. This method captures the laser-material interaction, thermal and fluid dynamics, and material solidification. By adjusting welding trajectories, the behaviour of the keyhole and melt pool formation is analyzed. To limit the number of experiments one of the simulation results are validated using experiments. The cut sections are used to validate the melt pool profile, and satisfactory correlation with the experiment results is observed. Additionally, this study investigates thermal and mechanical responses of hairpin windings in laser welded assemblies using FEM-thermo-mechanical and coupled electric-thermal-structural simulations. Six welding locations were analyzed, with cooling simulations revealing heat transfer, thermal stresses, and distortions near constraints. When a 300 A, 20 kHz alternating current was applied, different air cooling strategies showed that forced convection achieved lower and more stable temperatures and deformation than natural convection. The results highlight the need for thicker internal connectors and enhanced support to withstand high temperatures and deformation during operation.

Keywords: Laser welding, Simulation, Keyhole

## INTRODUCTION

The application of hairpin windings in electric vehicles has recently gathered increasing attention due to higher efficiency and power density of hairpin windings [1]. A complex manufacturing process involving laser welding is required to connect the hairpin couples, which can lead to issues such as porosity and spatter. To address these challenges and improve weld quality, extensive experimental and simulation studies have been conducted. Experimental investigations employing different laser sources and welding modes have focused on Cu-Cu hairpin contact welding. Ortolani et al. [2] investigated the geometry of the weld track and weld seam using a high-power blue laser (3 KW). This study demonstrated that a high-power blue diode laser can effectively weld copper hairpin windings using conduction mode, resulting in welds with low porosity and reduced spatter. However, the process is slower than the traditional keyhole welding. J. Ning et al. [3] investigated the effects of laser welding parameters and ultrasonic field parameters on copper hairpin joints. They concluded that laser spot welding under argon protection produces well-formed joints with good repeatability, while the closed scanning path enhances weld bead quality. Additionally, increasing ultrasonic power compresses the molten pool, reducing weld width. Haubold et al. [4] explored laser welding of copper using a novel high-power green disc laser. They used a full-factorial experimental design to identify thresholds between heat conduction and deep penetration welding. Results showed that vapor plume management is critical for stable deep penetration welding, while defocused green beams allow control over weld seam width in heat conduction mode. D'Arcangelo et al. [5] systematically compared the performance of conventional Gaussian beams with novel beam shapes, such as top-hat and annular profiles, across various wavelengths including infrared, green, and ultraviolet. The research assessed key parameters including weld morphology, mechanical strength, electrical resistance, and thermal efficiency. Findings indicated that certain beam shapes and wavelengths offer enhanced energy coupling and reduced thermal gradients, leading to improved weld quality and consistency. The paper provides valuable insights for optimizing laser welding processes in the manufacturing of electric motor components, aiming to enhance performance and reliability. Omlor et al. [6] investigated the influence of laser beam welding (LBW) parameters on the quality of hairpin windings in electric drives. They analyzed the effects of variables such as focus position, feed rate, laser power, oxygen content, and beam shaping on weld seam geometry, spatter formation, and porosity. They found that beam shaping reduced spatter and improved seam stability, while feed rate and focus position significantly impacted penetration depth and seam geometry. Dimatteo et al. [7] investigated the influence of laser power and welding speed on the morphology, mechanical strength, and electrical resistance of continuous-wave laser-welded pure copper hairpins. They found Optimal process parameters at an energy density of 11-12 MJ/cm², which produced welds with low porosity (<1%), high tensile strength, and reduced electrical resistance. Zhang et al. [8] investigated the effects of double-pass welding and extrusion techniques on the mechanical and microstructural properties of fiber laser welded 1.5-mm thick T2 copper

joints. They found that double-pass welding improved joint quality by reducing defects and enhancing mechanical performance compared to single-pass approaches. Yu et al. [9] presented a laser welding method for copper hairpin windings that incorporated visual recognition - utilizing a combination of Hough line detection and K-Means clustering algorithms - to detect and quantify gaps and lateral displacements after clamping. Four specific laser scanning trajectories were designed to match four distinct clamping scenarios. Experimental results demonstrate that by adjusting process parameters, similar weld morphology can be achieved across all scenarios, though the presence of gaps and displacements increases spatter and resistance, while decreasing tensile strength.

To deepen the understanding in various laser welding processes, an extensive comparative analysis of experiments is required, and these experiments require a considerable amount of time and investment. Consequently, digitalization of laser welding process through numerical simulations becomes essential. This approach can reduce experimental costs and duration, thereby reducing time to market. Initially various researchers used FEM-simulations to digitalize the laser welding simulations. Murua et al. [10] introduced a novel multiscale thermomechanical model for Laser Beam Welding (LBW), which automatically adapts the laser heat source to the welding regime, enhancing computational efficiency. Validated through experimental tests, the model accurately predicts welding regimes and vertical deformation, proving effective for LBW modeling. Fleischer et al. [11] focused on the numerical simulation of the hairpin welding process. They introduced a model-based approach using finite element simulations to analyze the influence of heat input during laser welding process. By simplifying the heat transfer problem, the study aimed to optimize welding parameters such as energy input rate and stripping length, reducing material costs and installation space. In the end, they highlighted the importance of early-stage numerical simulations in enhancing production-oriented design and mitigating economic risks in electric mobility.

The FEM simulations discussed here are effective for predicting temperature and deformation during the laser welding process. However, to further optimize laser welding process by examining melt pool dynamics, keyhole formation and stability, as well as metal vaporization and the solid-liquid phase transformation, it is essential to implement advanced numerical CFD simulations. Chianese et al. [12-13] used CFD-simulations to explore different laser welding strategies for dissimilar metal with focus on Cu-to-steel interfaces relevant to battery pack manufacturing. They investigated the impact of laser beam shaping, laser beam wobbling and part-to-part gap in laser welding process. For this, a multi-physics CFD simulation model was developed and validated against experimental data. The CFD model provided critical insights into temperature distribution, heat transfer, and melt behavior under varying welding conditions. They highlighted the importance of adapting laser parameters-beam shape, wobble frequency, and power distribution-to stabilize the keyhole, manage thermal gradients, and control mixing in dissimilar material welding. Satyanarayana et al. [14] demonstrated the effectiveness of using CFD simulations combined with the Taguchi method to optimize laser beam welding parameters. The integration of computational welding mechanics, including CFD and finite element models, showed good potential for predicting the thermal, mechanical, and microstructural behavior in welds.

## SIMULATION SETUP

The purpose of this study is to model and analyze the behavior of copper wires during laser welding process and its impact during the product application. This study focuses on developing a digital process chain with the help of multiple simulation software. The simulations were conducted sequentially, starting with a melt pool CFD analysis in Cradle CFD software, followed by a thermomechanical analysis in Simufact Welding software, and concluding with a coupled electric thermal structural Multiphysics analysis in LS DYNA. It must be noted that authors used an in-development feature of scSTREAM (cradle) software, which is not yet officially released. Authors have access to it, due to being part of Cradle software beta testing program. For the other simulations (thermomechanical analysis and coupled electric thermal structural), latest version of software was used.

### MELT POOL CFD ANALYSIS

The CFD analysis focused on a simplified two-wire copper hairpin model to investigate melt pool behavior. The mesh (Fig. 1.a) comprised of 1,116,000 elements with a finer resolution of 34 micrometers within the trajectory boundary and up to 3 millimeters in depth. Copper material properties, including multiple phases, were assigned to the wire. Initial conditions assumed room temperature and a fully solid phase for both the copper wires. Boundary conditions included no-slip boundaries at all fluid interfaces, conduction between solids, log-law heat transfer at fluid-solid boundaries, and adiabatic conditions at the outer boundary. The laser energy source, with a circular cross-section, had a power of 6000W and a speed of 650 mm/s.

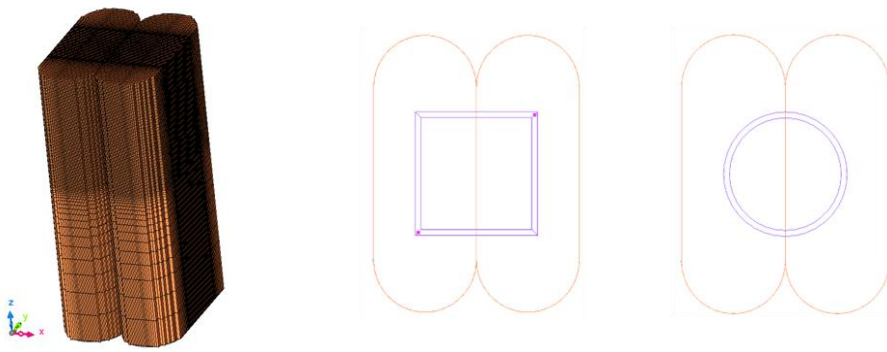

(a) (b) (c)

**Fig. 1** (a) The melt pool CFD analysis simulation setup with copper wires meshed at a finer resolution of 34 micrometers within the trajectory boundary and up to 3 millimeters in depth. (b) The square trajectory followed by the laser beam. (c) The circular trajectory followed by the laser beam

The melt pool and keyhole dynamics were simulated using a Multiphysics CFD framework implemented in Cradle CFD. The model solves the conservation equations of mass, momentum, and energy using a one-fluid formulation with free-surface capturing based on the multi-interface advection and reconstruction solver (MARS). Keyhole formation is modelled by incorporating recoil pressure arising from material evaporation at the liquid–gas interface. Multiple laser reflections within the keyhole are considered, enabling realistic prediction of energy concentration and keyhole stability. Fluid flow within the molten pool is driven by surface tension gradients, and Marangoni convection is explicitly included to capture thermocapillary effects influencing melt pool circulation and keyhole instability. In the present implementation, laser absorptivity is assumed constant and is not modelled as a function of temperature or surface condition. While evaporation-driven recoil pressure is considered, explicit porosity formation and stable void retention are not yet predicted.

Two cases were set up: one with a square-shaped laser trajectory (Fig. 1.b) and another with a circular-shaped trajectory (Fig. 1.c). The laser beam followed specified trajectories in multiple passes.

## THERMOMECHANICAL ANALYSIS

The second simulation involved a component-level thermomechanical analysis of the complete copper winding assembly, incorporating boundary conditions representing constraints used during the laser welding process (Fig. 2.a). Copper material properties were assigned to the windings, and fixed boundary conditions were applied. The laser energy source, with a circular cross-section, had a power of 6000W and a speed of 650 mm/s.

The transient temperature fields corresponding to the melt pool obtained from the CFD analysis were mapped as a volumetric heat source input (Fig. 2.b) into the thermomechanical welding simulation performed using Simufact Welding. The material behaviour was described using a temperature-dependent elastoplastic constitutive model with isotropic hardening, accounting for thermal expansion and phase-dependent material properties.

The square laser trajectory (Fig. 2.c) was chosen due to its superior weld quality. Welding was performed sequentially at six locations in the assembly.

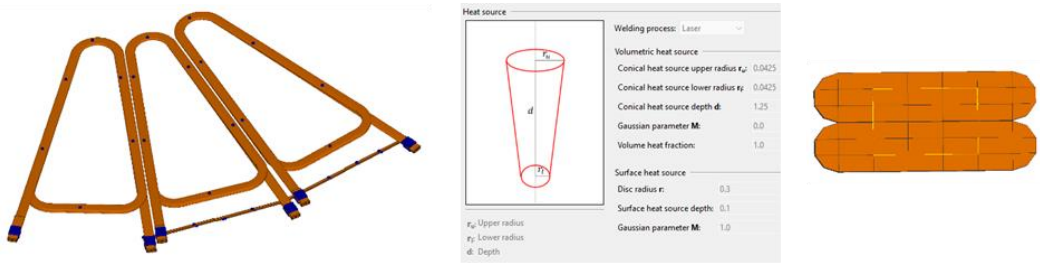


(a) (b) (c)

**Fig. 2** (a) Thermomechanical simulation set up with fixed boundary conditions (blue points). (b) Heat source parameter definition in Simufact welding for one of the passes. (c) Cross section view with the trajectory path (yellow line)

## COUPLED ELECTRIC THERMAL STRUCTURAL ANALYSIS

The third simulation assessed the impact of the laser welding process (presence of weld bead) on the application involving current flow through copper wires. The copper windings assembly, including weld beads and appropriate constraints, was subjected to a high-frequency 3-phase AC current (Fig. 3.a & Fig. 3.b). The loading condition was an alternating current of 300A with a frequency of 20KHz (Fig. 3.c).

Joule heating due to electrical current flow was coupled with structural response, enabling assessment of thermo-mechanical stresses during operational conditions. The coupling was performed in a sequential manner, where thermal fields influenced the mechanical response, consistent with standard industrial practice. This Multiphysics methodology in LS DYNA [15] enabled the computation of current flow through the copper wires, leading to resistive heating, increased temperature, thermal stress, and mechanical distortions. Simulations were conducted with two different convection heat transfer coefficients to evaluate cooling methods (free and forced air cooling) for optimizing thermal management strategies.

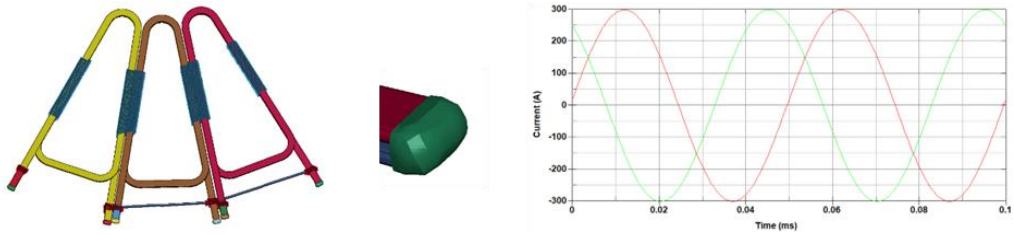


(a) (b) (c)

**Fig. 3** (a) Simulation set up for the coupled electric thermal mechanical multi physics analysis with high frequency 3 phase AC. (b) Weld bead model. (c) Input 3-phase current with maximum amplitude 300A and frequency of 20kHz

All the simulations (melt pool CFD analysis, thermomechanical analysis and coupled electric thermal structural analysis) were conducted on HP Z8 Fury G5 Workstation with processor Intel(R) Xeon(R) w5-3435X and 128 GB RAM computer.

## SIMULATION RESULTS

This section presents the results and inferences from the simulations. The findings are discussed in detail, comparing the weld bead quality from different trajectories with respect to melt pool formation. Additionally, the thermomechanical impacts on the copper wires during the laser welding process and the Multiphysics impacts during the current-carrying application are analyzed. The results provide insights into melt pool formation, thermal stresses, and mechanical distortions during the welding process, as well as their impact on performance. The effectiveness of different cooling strategies and the need for optimized connection designs are highlighted.

### MELT POOL CFD ANALYSIS

The CFD analysis compares two cases with different trajectories: a square trajectory with sides of 1.7 millimeters (Fig. 4.a - Fig. 4.g) and a circular trajectory with a diameter of 1.7 millimeters (Fig. 5.a - Fig. 5.g). The laser beam traveled these trajectories six times and melt pool development was captured at the end of each pass.

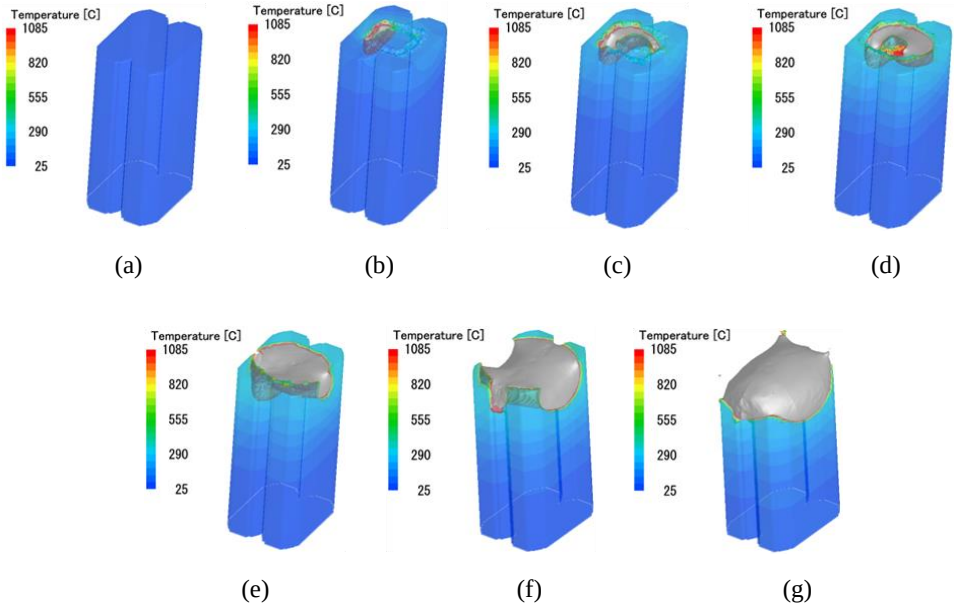


**Fig. 4** Melt pool development with the square trajectory at the end of each pass (a)0s. (b) 0.01s. (c) 0.021s. (d) 0.031(s). (e) 0.042s. (f) 0.052s. (g) 0.063s

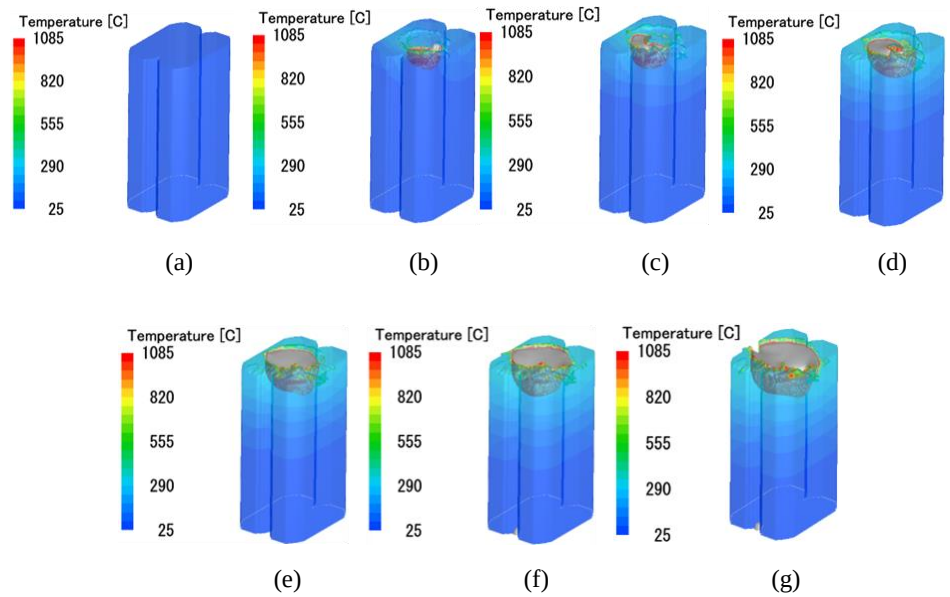


**Fig. 5** Melt pool development with the circular trajectory at the end of each pass (a)0s. (b) 0.008s. (c) 0.016s. (d) 0.025(s). (e) 0.033s. (f) 0.041s. (g) 0.050s

The comparison revealed better melt formation with the square trajectory, resulting in a dome-shaped melt pool. The circular trajectory was shorter, imparting less energy to the copper wires. To eliminate this difference in comparison, the laser beam continued the trajectory for eight passes. The comparison showed that the square trajectory still performed better than the circular trajectory. The square trajectory, being closer to the edges of the copper wire, allowed faster heat transfer to the edges and subsequently faster melting (Fig. 6.a - Fig. 6.c). In contrast, the circular trajectory was more confined to the center region and failed to melt the corner regions, which were important for dome shape formation (Fig. 6.d - Fig. 6.f).

A cut-section view through the center of both copper wires measured maximum melt pool depth at several data points (Fig. 7.a). The plot indicated consistently higher melt pool depth for the square trajectory compared to the circular trajectory (Fig. 7.b).

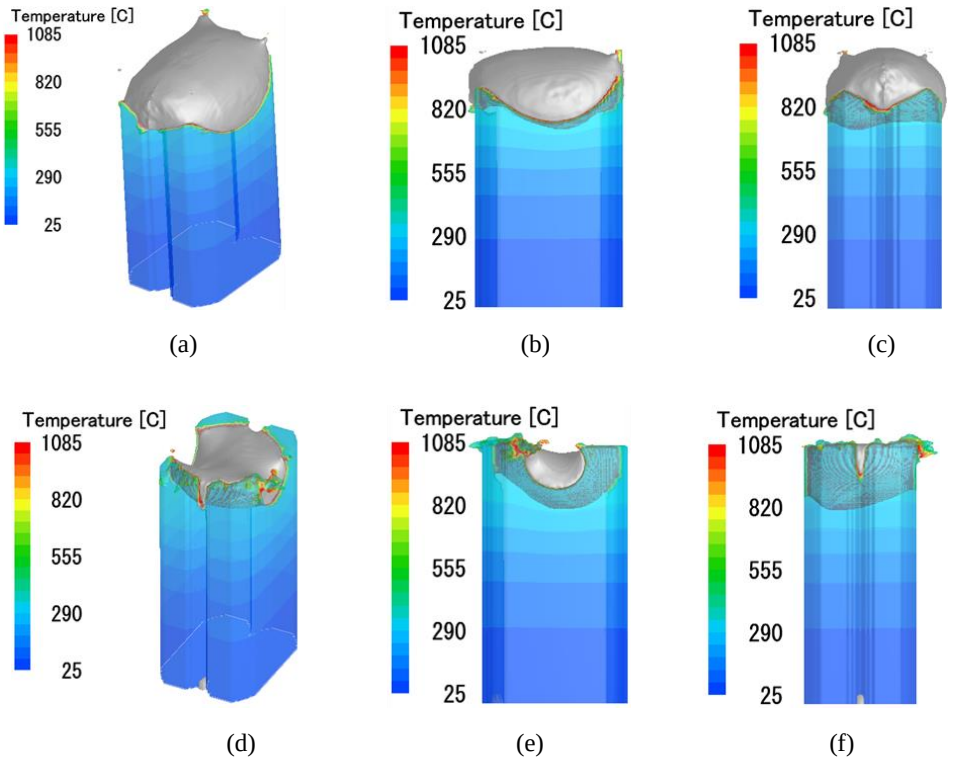


**Fig. 6** The melt pool comparison at the end of 0.063s. Square trajectory completed 6 passes (a) Isometric view. (b) Front view. (c) Side view. Circular trajectory covering the 8$^{th}$ pass (d) Isometric view. (e) Front view. (f) Side view

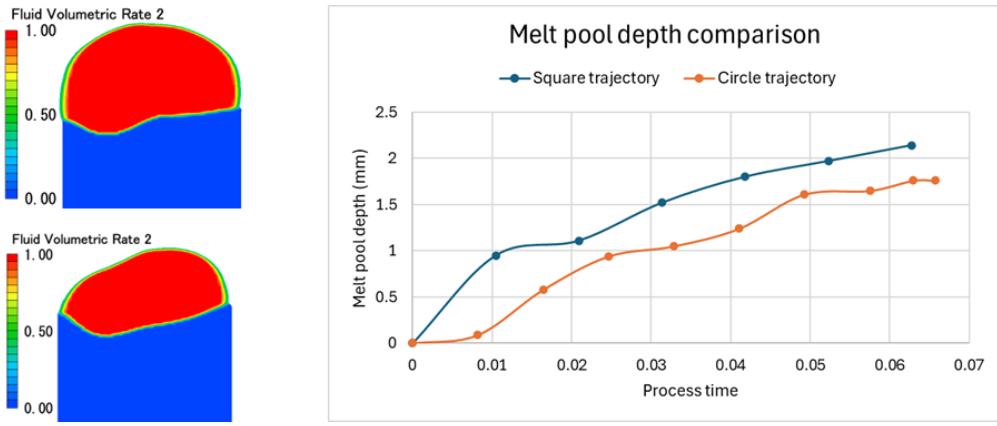


(a) (b)

**Fig. 7** The melt pool depth measured at different times corresponding to the end of each pass. (a) The top image corresponds to square trajectory and bottom image corresponds to circular trajectory. (b) Melt pool depth comparison between square and circular trajectory

Laser material interaction (Fig. 8.a) was assessed to understand laser energy absorption during the process. The average laser energy absorbed was higher with the square trajectory by approximately 20%, explaining the superior weld quality (Fig. 8.b).

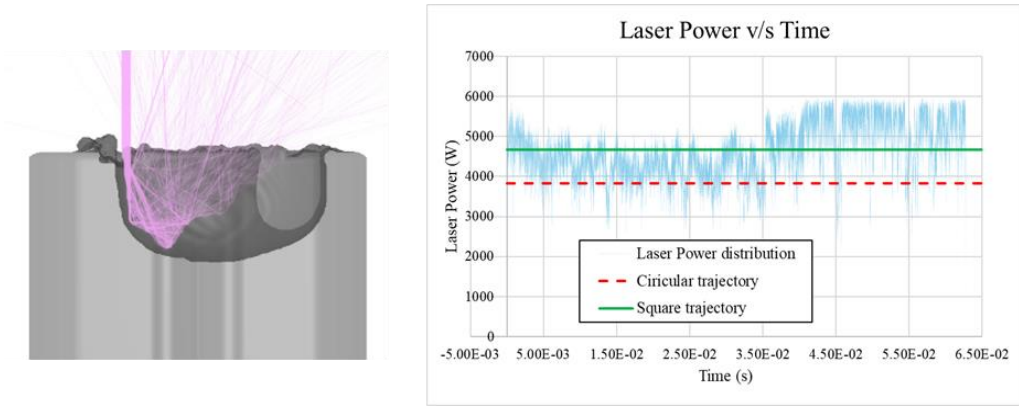


(a) (b)

**Fig. 8** (a) Laser material interaction where laser goes through multiple reflections. (b) Average laser power absorption comparison between square and circular trajectory

## THERMO-MECHANICAL ANALYSIS

The square trajectory was chosen for thermomechanical analysis due to its better weld quality. Maximum melt pool depth at the end of each pass was extracted and scaled to define the heat source volume for each pass in the thermomechanical simulation. The average melt pool depth at each pass closely matched observations from the CFD analysis (Fig. 9.a). The analysis consisted of laser welding processes at 6 locations, 3 connecting the windings to the 3-phase inputs and another 3 for interconnection between the windings.

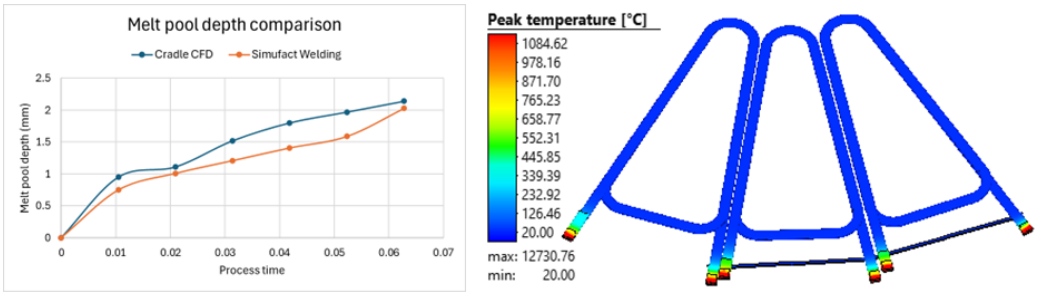


(a) (b)

**Fig. 9** (a) The melt pool depth comparison between Simufact Welding and Cradle CFD, validating the thermomechanical model. (b) Windings peak temperature (°C) at the end of six welding process (zoomed in image at top right): 3 connecting the 3-phase wires to the windings and 3 providing interconnection between the windings

The second part of the simulation involved cooling hairpin windings at atmospheric conditions, leading to heat transfer by conduction and convection, and formation of thermal stresses and distortions near the fixed boundary conditions. Higher stresses were observed close to the locations where the constraints were provided (Fig. 10.b).

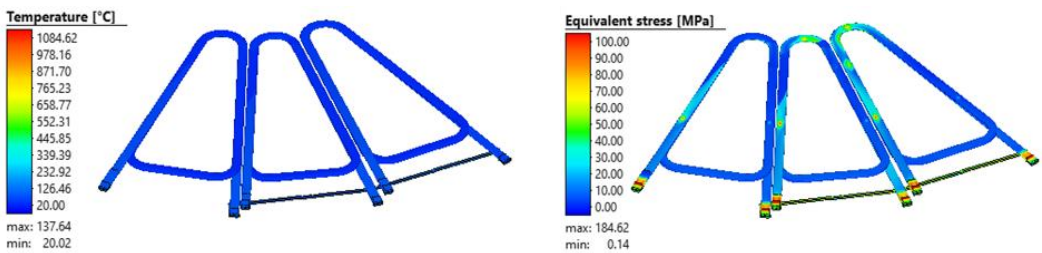


**Fig. 10** (a) The model cooled down to room temperature (°C) with natural atmospheric cooling. (b) Stress formation observed near the constrained locations

## COUPLED ELECTRIC THERMAL STRUCTURAL ANALYSIS

Weld bead models, based on the melt pool shape from the CFD analysis, were used as connections at six locations in the windings' assembly via tied contact option. An electric current of 300A with a frequency of 20kHz was passed through the windings assembly, resulting in alternating current through each winding over time (Fig. 11).

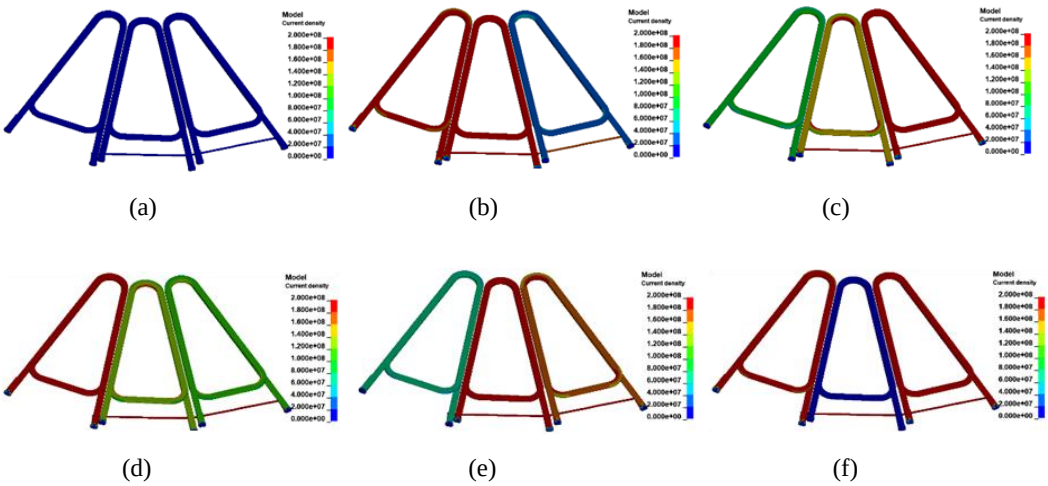


**Fig. 11** The alternating current flow (current density in A/mm²) through the copper wires at different times (a) 0ms. (b) 0.01ms. (c) 0.02ms. (d) 0.03ms. (e) 0.04ms. (f) 0.05ms

The current flow through the windings increased the temperature due to resistive heating of the copper wires, causing thermal stress as the windings were constrained at different locations, restricting thermal expansion. Two simulations with different cooling conditions, natural air cooling (H=10 W/m²K) and forced air cooling (H=100 W/m²K), were performed to optimize thermal management strategies. The current flowed through the windings for three minutes, with forced air cooling reaching thermal equilibrium at 480K in approximately 80 seconds, while natural convection did not reach equilibrium with a temperature of approximately 1500K in 180 seconds. The winding interconnections showed high temperature readings with the forced convection model reaching an equilibrium temperature of 1600K while the natural convection model couldn't attain equilibrium at a temperature of 9000K in 180 seconds.

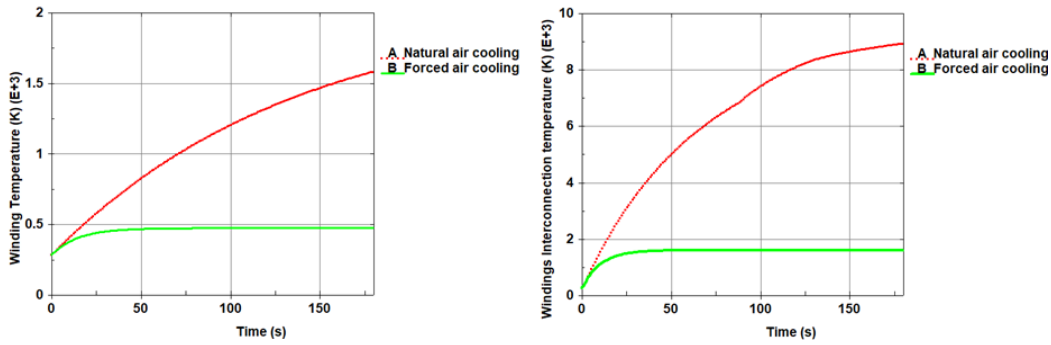


(a) (b)

**Fig. 12** (a) Windings temperature comparison with natural and forced air cooling. (b) Windings interconnection temperature comparison with natural and forced air cooling

High temperatures and subsequently high deformations were observed in the connector providing internal connections between the three windings in both cases, suggesting design change requirements with thicker internal connections and higher structural support for them during current flow application. Comparatively the forced convection model performed better compared to the natural convection model with a lower level of deformation for the same support conditions.

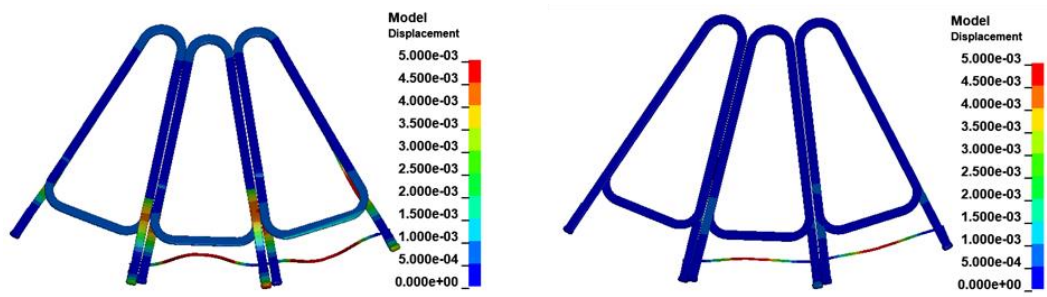


**Fig. 13** The windings internal connections experienced high deformation due to thermal expansion at high temperatures for (a) natural air cooling (b) forced air cooling

## EXPERIMENTAL SETUP AND RESULTS

Copper hairpin specimens with a rectangular cross section measuring 1.5 mm × 4 mm were fabricated from high-purity copper (purity: 99.9%). The experimental setup utilized an infrared laser source with a wavelength of 1060 μm and a beam diameter of 50 μm. Laser processing was conducted at a power of 6000 W and a scanning speed of 650 mm/s. The

laser was programmed to follow a square trajectory, each side measuring 1.7 mm, consistent with the conditions used in corresponding simulation studies.

To ensure experimental reproducibility and reliability, six copper hairpin samples were processed under identical conditions. For each specimen, cross-sectional images were analyzed to assess and document the weld morphology. The results demonstrated high consistency, with analogous structural features observed across all specimens. A representative cross-sectional image is presented to show the experimental findings.

Fig. 1 presents the microstructural characteristics of the welded copper hairpin strips. It can be observed that the maximum melt pool depth on the left side attains 2711µm, exceeding the depth measured on the right side. This asymmetry is due to the initiation of the laser scanning from the left, resulting in prolonged exposure to elevated temperatures and increased localized heat accumulation, thereby producing a deeper melt pool. Additionally, small pores are visible in the cross-sectional micrograph, which are typically attributed to rapid solidification phenomena inherent to laser welding of copper.

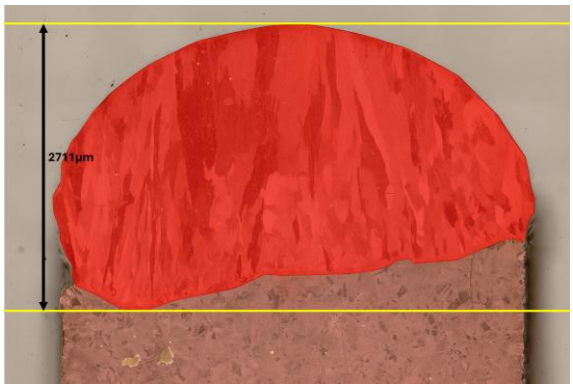


**Fig. 13** Cross-section image of square trajectory

A comparative analysis of Fig. 13 with the simulation results (Fig. 7.a top) reveals a strong correlation between the experimentally measured melt pool geometries and the computational fluid dynamics (CFD) simulation predictions, thereby validating the numerical approach employed in this investigation.

## CONCLUSION

This study examines laser welding in copper hairpin windings using both multiphysics simulations and experimental validation. CFD analyses compared melt pool development for 1.7 mm square and circular laser trajectories across multiple passes. The square trajectory produced superior melt pools - deeper, more uniform, and dome-shaped - due to better thermal distribution and about 20% greater laser energy absorption. Thermomechanical simulations, supported by CFD, showed that the square path reduced thermal stresses and

mechanical distortions. Coupled electric-thermal-structural simulations evaluated current-carrying performance. Forced air cooling (H=100 W/m²K) enabled thermal equilibrium at 480 K in roughly 80 seconds. Natural convection failed to stabilize, with temperatures reaching 1500 K in 180 seconds. High stresses and deformations were observed at internal winding connections, indicating a need for thicker, better-supported connectors. Experimental tests used six high-purity copper hairpin samples and a 6000 W infrared laser following square trajectories. Cross-sectional analysis revealed consistent weld morphology and deeper melt pools on the weld initiation side. These results closely matched CFD predictions. Minor porosity, typical of rapid copper solidification, was also observed. The findings highlight the influence of laser trajectory and cooling strategy on weld quality, thermal management, and mechanical reliability. The validated simulation approach provides a strong foundation for optimizing laser welding.

## ACKNOWLEDGEMENTS

Authors like to express their sincere appreciation to the Cradle support team for their invaluable assistance in the simulation work undertaken for this research. Their technical expertise, prompt guidance, and unwavering support greatly contributed to the successful completion of the study.

## References

[1] A. RIEDEL, M. MASUCH, M. WEIGELT, T. GLÄSEL, A. KÜHL, S. REINSTEIN and J. FRANKE: 'Challenges of the Hairpin Technology for Production Techniques', *21st International Conference on Electrical Machines and Systems (ICEMS)*, Vol. 21, pp. 2471-2476, 2018.

[2] M. ORTOLANI, G. BORZONI, D. NOCCIOLINI, B. PREVITALI and A. G. DEMIR: 'Conduction mode welding of Cu hairpins with a 3-kW blue laser with external features correlated to quality attributes', *The International journal of Advanced Manufacturing Technology,* 137, pp. 1959-1974, 2025.

[3] J. NING and L. ZHANG: 'Non-contact ultrasonic-assisted laser welding of copper hairpins', *journal of Materials Research and Technology,* Vol. 31, pp. 3536-3550, 2024.

[4] M. HAUBOLD, A. GANSER, T. EDER and M. F. ZÄH: 'Laser welding of copper using a high power disc laser at green wavelength', *10th CIRP Conference on Photonic Technologies*, Vol. 74, pp. 446-449, 2018.

[5] S. D'ARCANGELO, L. CAPRIO, D. CHESI, D. NOCCIOLINI, R. CORBINELLI, B. PREVITALI and A. G. DEMIR: 'Comprehensive benchmarking of laser welding technologies including novel beam shapes and wavelengths for e-drive copper hairpins', *Optics & Laser Technology*, Vol. 169, 10964, 2024.

[6] M. OMLOR, N. SEITZ, T. BUTZMANN, T. PETRICH, R. GRÄF, A. HESSE and K. DILGER: 'Quality characteristics and analysis of input parameters on laser beam welding of hairpin windings in electric drives', *The International Journal of Materials Joining*, Vol. 67, pp. 1491-1508, 2023.

[7] V. DIMATTEO, A. ASCARI, P. FAVERZANI, L. POGGIO and A. FORTUNATO: 'The effect of process parameters on the morphology, mechanical strength and electrical resistance of CW laser-welded pure copper hairpins', *Journal of Manufacturing Processes*, Vol. 62, pp. 1491-1508, 2021.

[8] J. NING, L. ZHANG, A. WANG, Q. BAI, J. YANG and J. ZHANG: 'Effects of double-pass welding and extrusion on properties of fiber laser welded 1.5-mm thick T2 copper joints', *Journal of Materials Processing Technology*, Vol. 237, pp. 75-87, 2016.

[9] H. YU, Y. YIN, S. JI, C. ZHANG, T. ZHU and Z. LIU: 'Laser welding method and quality analysis of hairpin windings based on visual recognition of gap and displacement matching process', *Optics & Laser Technology*, Vol. 178, 111224, 2024.

[10] O. MURUA, J. ARRIZUBIETA, A. LAMIKIZ and H. SCHNEIDER: 'Numerical simulation of a laser beam welding process: From a thermomechanical model to the experimental inspection and validation', *Thermal Science and Engineering Progress*, Vol. 55, 102901, 2024.

[11] J. FLEISCHER, L. HAUSMANN and F. WIRTH: 'Production-oriented design of electric traction drives with hairpin winding', *31st CIRP Design Conference*, Vol. 100, pp. 169-174, 2021.

[12] G. CHIANESE, S. JABAR, P. FRANCIOSA, D. CEGLAREK and S. PATALANO: 'A multi-physics CFD study on the part-to-part gap during remote laser welding of copper-to-steel battery tab connectors with beam wobbling', *12th CIRP Conference on Photonic Technologies*, Vol. 111, pp. 484-489, 2022.

[13] G. CHIANESE, Q. HAYAT, S. JABAR, P. FRANCIOSA, D. CEGLAREK and S. PATALANO: 'A multi-physics CFD study to investigate the impact of laser beam shaping on metal mixing and molten pool dynamics during laser welding of copper to steel for battery terminal-to-casing connections', *Journal of Materials Processing Technology*, Vol. 322, 118202, 2023.

[14] G. SATYANARAYANA, K. NARAYANA and B. N. RAO: 'Incorporation of Taguchi approach with CFD simulations on laser welding of spacer grid fuel rod assembly', *Materials Science and Engineering: B*, 137, Vol. 269, 115182, 2021.

[15] M. SREEJITH AND P. RANA: 'Integrated Electrical-Thermal-Structural Analysis in High-Frequency AC Systems Using LS-DYNA', *ANSYS Innovation Conference*, Germany, 2024.